Journal of Biomolecular NMR (2005) 33: 163–174
DOI 10.1007/s10858-005-3472-7
© Springer 2005

Article

Determination of ^{13}C CSA tensors: Extension of the model-independent approach to an RNA kissing complex undergoing anisotropic rotational diffusion in solution

Sapna Ravindranathan[a,*], Chul-Hyun Kim[b] & Geoffrey Bodenhausen[c,d]
[a]*Central NMR Facility, National Chemical Laboratory, Dr. Homi Bhabha Road, Pune, 411008 India;* [b]*Department of Chemistry and Biochemistry, California State University, Hayward, 25800 Carlos Bee Boulevard, Hayward, CA, 94542-3089 USA;* [c]*Institut des Sciences et Ingénierie Chimiques, Ecole Polytechnique Fédérale de Lausanne, BCH, 1015 Lausanne, Switzerland;* [d]*Département de Chimie, associé au CNRS, Ecole Normale Supérieure, 24, rue Lhomond, 75231 Paris Cedex 05, France*

Received 26 May 2005; Accepted 19 September 2005

Key words: anisotropic rotational diffusion, chemical shift anisotropy tensors, cross-correlation, model-independent approach, NMR

Abstract

Chemical shift anisotropy (CSA) tensor parameters have been determined for the protonated carbons of the purine bases in an RNA kissing complex in solution by extending the model-independent approach [Fushman, D., Cowburn, D. (1998) *J. Am. Chem. Soc.* **120**, 7109–7110]. A strategy for determining CSA tensor parameters of heteronuclei in isolated X–H two-spin systems (X = ^{13}C or ^{15}N) in molecules undergoing anisotropic rotational diffusion is presented. The original method relies on the fact that the ratio $\kappa_2 = R_2^{auto}/R_2^{cross}$ of the transverse auto- and cross-correlated relaxation rates involving the X CSA and the X–H dipolar interaction is independent of parameters related to molecular motion, provided rotational diffusion is isotropic. However, if the overall motion is anisotropic κ_2 depends on the anisotropy $D_{||}/D_{\perp}$ of rotational diffusion. In this paper, the field dependence of both κ_2 and its longitudinal counterpart $\kappa_1 = R_1^{auto}/R_1^{cross}$ are determined. For anisotropic rotational diffusion, our calculations show that the average $\kappa_{av} = 1/2\ (\kappa_1 + \kappa_2)$, of the ratios is largely independent of the anisotropy parameter $D_{||}/D_{\perp}$. The field dependence of the average ratio κ_{av} may thus be utilized to determine CSA tensor parameters by a generalized model-independent approach in the case of molecules with an overall motion described by an axially symmetric rotational diffusion tensor.

Introduction

Chemical shift tensors are remarkably sensitive to electronic structure and intermolecular interactions. Several studies have shown interesting correlations between biomolecular structures and chemical shifts (Sitkoff and Case, 1998). In proteins, for example, C^{α} chemical shifts correlate with the backbone dihedral angles ψ and ϕ and help to identify secondary structure elements (Spera and Bax, 1991; Szilagyi, 1995). In nucleic acids, the chemical shift of the sugar carbon C1′ correlates with the glycosidic torsion angle, thereby facilitating the identification of 'syn' and 'anti' conformations (Ghosh et al., 1994). The C3′ and C5′ chemical shifts are sensitive to the sugar pucker (Wijmenga and van Buuren, 1998). Often, much stronger variations are observed upon structural changes in the chemical shift anisotropy (CSA). It has been shown

*To whom correspondence should be addressed. E-mail: s.ravindranathan@.ncl.res.in

that the variation with secondary structure in the CSA at the C^{α} position is much larger than for the isotropic chemical shift (Tjandra and Bax, 1997b). Density functional theory calculations predict much larger changes in the chemical shift anisotropies compared to isotropic chemical shifts for the C1′ and C3′ carbons with changes in the pseudorotation angle defining the ribose conformation (Dejaegere and Case, 1998). The correlation between sugar pucker and the C1′ and C3′ chemical shift anisotropies have been experimentally demonstrated by $^{13}C/^{13}C$–^{1}H CSA/dipole cross-correlated relaxation rate measurements (Boisbouvier et al., 2000). Correlations between chemical shift anisotropies of the amide protons in proteins and the hydrogen bond length have been demonstrated by $^{1}H/^{15}N$–^{1}H CSA/dipole cross-correlated relaxation experiments (Tjandra and Bax, 1997a; Tessari et al., 1997). Ab initio studies on nucleic acid base pairs also predict variations in the imino ^{15}N and imino ^{1}H CSA tensors with changes in the hydrogen bond distance (Czerek, 2001).

Knowledge of CSA tensors is also important for the interpretation of relaxation experiments designed to characterize dynamics of biomolecules. Along with dipolar interactions, the CSA is a major source of relaxation at high magnetic field strengths. Most analyses of ^{15}N and ^{13}C relaxation rates in proteins and nucleic acids rely on CSA tensor information obtained from solid-state NMR studies or from ab initio calculations on small peptides, free nucleotide bases or related model compounds. Different approaches have also been adopted recently to determine CSA tensors of ^{15}N and ^{13}C nuclei involved in ^{15}N–^{1}H or ^{13}C–^{1}H bonds in proteins in solution. For example, ratios R_1^{auto}/R_2^{auto} of spin–lattice and spin–spin relaxation rates have been analyzed assuming fixed magnitudes of the principal components of the ^{15}N CSA tensor to examine variability in the orientation of this tensor in different residues of a protein (Boyd and Redfield, 1998). Another class of methods is based on measurements of chemical shift changes induced by weak alignment of biomolecules in a magnetic field or in liquid crystalline media (Ottiger et al., 1997; Cornilescu and Bax, 2000; Boyd and Redfield, 1999). Using this approach, average ^{15}N CSA tensor magnitudes and orientations have been determined for residues in α helix and β sheet regions. Interference effects between CSA and dipolar relaxation have also been utilized to estimate chemical shift anisotropy tensors (Tjandra and Bax, 1997b; Tjandra et al., 1996; Pang and Zuiderweg, 2000; Cisnetti et al., 2004; Ghosh et al., 1998). This method however requires the assumption of a motional model.

Recently, Fushman et al. have proposed an elegant procedure to determine CSA tensor parameters independently of motional models (Fushman and Cowburn, 1998; Fushman et al., 1998). This approach, originally demonstrated for ^{15}N nuclei of backbone ^{15}N–^{1}H groups in proteins, utilizes the fact that both the transverse auto-relaxation rate (R_2^{auto}) and the transverse CSA/dipole cross-correlation rate (R_2^{cross}) are dominated by the spectral density functions $J(0)$ and $J(\omega_N)$. The ratio R_2^{cross}/R_2^{auto} only depends on the ^{15}N–^{1}H dipolar interaction and ^{15}N CSA tensor and is independent of parameters relating to molecular motion, provided rotational diffusion is isotropic. From a field dependence of the ratio, parameters relating to the magnitude and orientation of the CSA tensor can be separated. A related approach using a combination of spin-lattice relaxation rates R_1^{auto} and the longitudinal CSA/dipole cross-correlation rate R_1^{cross} has been applied to determine the ^{13}C CSA parameters of a ^{13}C–^{1}H group in the aromatic ring of tyrosine (Damberg et al., 1999). The longitudinal CSA/dipole cross-correlation rate depends on the spectral density function $J(\omega_C)$. The ^{13}C spin–lattice relaxation rate $R_1^{auto}(C_z)$, ^{1}H spin-lattice relaxation rate $R_1^{auto}(H_z)$ and the relaxation rate of the longitudinal two spin order $R_1^{auto}(2C_zH_z)$ are measured to estimate $J(\omega_C)$, using $J(\omega_C) \propto R_{comb} = R_1^{auto}(C_z) + R_1^{auto}(H_z) - R_1^{auto}(2C_zH_z)$. The field dependence of the quantity $B_0 \times (R_{comb}/R_1^{cross})$ is then utilized to determine the ^{13}C tensor parameters. The approach based on longitudinal relaxation rates avoids errors associated with conformational exchange contributions to transverse relaxation and the approximation which discards high-frequency spectral density functions. More recently, a larger experimental data set consisting of ratios of both longitudinal and transverse relaxation rates have been analyzed jointly to examine variations in ^{15}N CSA magnitudes and orientations in Ubiquitin (Damberg et al., 2005). In the analysis, the effects of rotational anisotropy is accounted for by estimating a correction factor for the

experimental rates from calculations of theoretical relaxation rates using assumed values for the CSA tensors.

In this paper, we extend the approach proposed by Fushman et al. (1998) to determine ^{13}C CSA tensors of the protonated carbons of nucleotide bases in nucleic acids, with application to the RNA kissing complex shown in Figure 1. The ratio $\kappa_2 = R_2^{auto}/R_2^{cross}$ is cleanly separable into a product of a 'dynamic' factor and a 'structural' factor only if the overall motion of the molecule can be described by isotropic rotation. In general, when the number of base pairs in a nucleic acid exceeds ten, overall molecular tumbling starts to deviate significantly from isotropic motion. Here, we consider the ratio $\kappa_2 = R_2^{auto}/R_2^{cross}$ and its longitudinal counterpart $\kappa_1 = R_1^{auto}/R_1^{cross}$, discarding the high-frequency spectral density functions so that only $J(0)$ and $J(\omega_C)$ are taken into account for the transverse relaxation rates while for longitudinal relaxation rates we consider only $J(\omega_C)$. In this approximation, both ratios κ_1 and κ_2 should be identical for isotropic overall rotation. Numerical calculations of the two ratios carried out assuming axially symmetric anisotropic rotational diffusion show that even though the ratios individually depart from the values expected for isotropic rotation, the average $\kappa_{av} = 1/2\ (\kappa_1 + \kappa_2)$ is largely independent of the anisotropy $D_{||}/D_{\perp}$. It is thus possible to extend the model-independent approach for determining CSA tensor parameters to molecules which have a significantly anisotropic overall motion, by utilizing the average κ_{av} of the ratios determined from transverse and longitudinal relaxation rates.

Theory

We consider an isolated scalar coupled two-spin system ^{13}C–^{1}H. Relaxation of the ^{13}C spin is governed by the ^{13}C–^{1}H dipolar interaction and the ^{13}C CSA interaction with the static magnetic field. All relaxation rate constants can be expressed in terms of the spectral density function $J(\omega)$. The rate constant for auto-relaxation of the transverse magnetization (C_x,C_y) is given by (Abragam, 1961):

$$\begin{aligned} R_2^{auto} =& (d^2/20)[4J(0) + 3J(\omega_C) + J(\omega_H - \omega_C) \\ &+ 6J(\omega_H) + 6J(\omega_H + \omega_C)] + (1/45) \\ &\times (\Delta\sigma_{eff})^2\omega_C^2[4J(0) + 3J(\omega_C)] + R_{ex} \end{aligned} \quad (1)$$

The rate constant for auto-relaxation of the longitudinal magnetization (C_z) is given by (Abragam, 1961),

$$\begin{aligned} R_1^{auto} =& (d^2/10)[3J(\omega_C) + J(\omega_H - \omega_C) \\ &+ 6J(\omega_H + \omega_C)] + (2/15) \\ &\times (\Delta\sigma_{eff})^2\omega_C^2[3J(\omega_C)]. \end{aligned} \quad (2)$$

The dipolar interaction constant d is given by,

$$d = \left(\frac{\mu_0}{8\pi^2}\right)\frac{\gamma_C\gamma_H h}{r_{CH}^3}, \quad (3)$$

where γ_C and γ_H are the gyromagnetic ratios of ^{13}C and ^{1}H, μ_0 is the permeability of vaccuum, h is Planck's constant and r_{CH} is the internuclear distance. The CSA contribution to the relaxation rates depends on the magnitude of the CSA tensor and the ^{13}C Larmor frequency, $\omega_C = -\gamma_C B_0$, where B_0 is the static magnetic field. In general, the CSA tensor is not axially symmetric and the effective anisotropy $\Delta\sigma_{eff}$ contributing to the relaxation rates is defined as (Damberg et al., 1999; Czernek et al., 2000; Boisbouvier et al., 1999),

$$\Delta\sigma_{eff} = \sqrt{(\sigma_{11} - \sigma_{33})^2 + (\sigma_{22} - \sigma_{33})^2 - (\sigma_{11} - \sigma_{33})(\sigma_{22} - \sigma_{33})}, \quad (4)$$

where σ_{11}, σ_{22} and σ_{33} are the principal components of the CSA tensor. The transverse relaxation rate has an additional contribution R_{ex} in the case of conformational exchange.

Interference between the ^{13}C CSA and ^{13}C-^{1}H dipolar interactions can result in an interconversion of coherence or spin order. In the case of transverse relaxation, an initial coherence C_x may be converted to $2C_xH_z$. In longitudinal relaxation on the other hand, an initial magnetization C_z can be converted to two-spin order $2C_zH_z$. The transfer depends on $^{13}C/^{13}C$-^{1}H CSA/dipole cross-correlated relaxation

rates, which for transverse and longitudinal relaxation are given by (Goldman, 1984),

$$R_2^{\text{cross}} = -(1/15)d\Delta\sigma^*\omega_C[4J(0) + 3J(\omega_C)] \quad (5)$$

and

$$R_1^{\text{cross}} = -(1/15)d\Delta\sigma^*\omega_C[6J(\omega_C)], \quad (6)$$

respectively. In addition to the strengths of the spin interactions, these cross-correlation rates also depend on the orientation of the dipolar interaction with respect to the CSA tensor. For the general case of an asymmetric CSA tensor, the geometric dependence is included in the parameter $\Delta\sigma^*$ which is defined as (Boisbouvier et al., 1999; Brutscher, 2000),

$$\begin{aligned}\Delta\sigma^* =& P_2(\cos\theta_{11,CH})(\sigma_{11} - \sigma_{33}) \\ &+ P_2(\cos\theta_{22,CH})(\sigma_{22} - \sigma_{33}).\end{aligned} \quad (7)$$

The angles $\theta_{11,CH}$ and $\theta_{22,CH}$ which appear as arguments of the Legendre polynomials define the orientation of the ^{13}C–^{1}H vector with respect to the components 11 and 22 of the CSA tensor.

Assuming that the overall molecular motion can be described by isotropic rotation with a rotational diffusion constant D_{iso}, the spectral density function is given by (Abragam, 1961; Woessner, 1962),

$$J(\omega) = \frac{6D_{iso}}{(6D_{iso})^2 + \omega^2}, \quad (8)$$

D_{iso} is the average of the principal components of the rotational diffusion tensor and is related to the correlation time for isotropic rotation τ_c^{iso} by $D_{iso} = 1/6\tau_c^{iso}$.

In the case of a molecule undergoing anisotropic rotational diffusion with an axially symmetric diffusion tensor, the auto- and cross-correlated spectral density functions are given by (Tjandra et al., 1996; Woessner, 1962; Richter et al., 1999),

$$\begin{aligned}J_{uv}(\omega) =& \frac{1}{4}(3\cos^2\theta_u - 1)(3\cos^2\theta_v - 1)\left(\frac{6D_\perp}{(6D_\perp)^2 + \omega^2}\right) \\ &+ 3\cos\theta_u\cos\theta_v\sin\theta_u\sin\theta_v\cos(\phi_u - \phi_v)\left(\frac{5D_\perp + D_\parallel}{(5D_\perp + D_\parallel)^2 + \omega^2}\right), \\ &+ \frac{3}{4}\sin^2\theta_u\sin^2\theta_v\cos(2\phi_u - 2\phi_v)\left(\frac{2D_\perp + 4D_\parallel}{(2D_\perp + 4D_\parallel)^2 + \omega^2}\right)\end{aligned} \quad (9)$$

where $D_{||}$ and $D_\perp$ are related to the principal components of the rotational diffusion tensor as $D_{||} = D_{zz}$ and $D_\perp = D_{xx} = D_{yy}$. For the auto-correlation spectral density functions in Equations (1) and (2), $u = v$. For spectral density functions in Equations (5) and (6) $u \neq v$ since the rates correspond to cross-correlation functions involving two distinct spin interactions. The polar angles (θ_u, ϕ_u) and (θ_v, ϕ_v) define the orientations of these spin interactions in the frame of the rotational diffusion tensor.

In the case of biological macromolecules at high magnetic fields, the spectral density functions involving high frequency terms, $J(\omega_H + \omega_C)$, $J(\omega_H - \omega_C)$ and $J(\omega_H)$ are small compared to $J(0)$ and $J(\omega_C)$ and can be neglected to a first approximation. The transverse auto-relaxation rate constant R_2^{auto} and cross-correlation rate constant R_2^{cross} are then both proportional to $[4J(0) + 3J(\omega_C)]$. In spin systems which do not have any conformational exchange contribution R_{ex} to transverse relaxation, the ratio $\kappa_2 = R_2^{auto}/R_2^{cross}$ is therefore independent of the correlation time of isotropic tumbling. On the other hand, the longitudinal auto-relaxation rate constant R_1^{auto} and cross-correlation rate constant R_1^{cross} are both proportional to $J(\omega_C)$ so that the ratio $\kappa_1 = R_1^{auto}/R_1^{cross}$ does not depend on correlation time either. In this case, one also avoids possible effects of conformational exchange. Assuming that the molecule undergoes isotropic rotation and that contributions R_{ex} from chemical exchange can be neglected, the ratios $\kappa_1 =$

R_1^{auto}/R_1^{cross} and $\kappa_2 = R_2^{auto}/R_2^{cross}$ are both given by,

$$\kappa_{iso} = \frac{9d^2 + 4\gamma_C^2 B_0^2 \Delta\sigma_{eff}^2}{12 d \gamma_C B_0 \Delta\sigma^*} \quad (10)$$

As shown by Fushman et al. (1998) the various relaxation rates can be measured at different magnetic field strengths and the CSA parameters $\Delta\sigma_{eff}$ and $\Delta\sigma^*$ may be determined from the field dependence of either κ_1 or κ_2. In this paper, we extend this approach to systems with anisotropic rotational motion. We demonstrate that the average $\kappa_{av} = 1/2(\kappa_1 + \kappa_2)$ coincides with κ_{iso} and is largely independent of $D_{||}/D_{\perp}$, so that $\Delta\sigma_{eff}$ and $\Delta\sigma^*$ may be determined from the field dependence of κ_{av}.

Materials and methods

The ^{13}C relaxation rate measurements were performed using Bruker spectrometers operating at three different field strengths corresponding to proton resonance frequencies of 600, 400 and 300 MHz. The longitudinal and transverse ^{13}C relaxation rates (R_1^{auto} and R_2^{auto}) were measured from a series of heteronuclear ^{13}C–^{1}H correlated spectra employing previously reported pulse sequences (Kay et al., 1992). Data sets were recorded at 600 MHz using delay times T = 4.2, 8.6, 12.9, 17.2, 21.5, 25.6, 30.0 and 34.3 ms for R_2^{auto} and 40, 80, 160, 240, 480, 800 and 1000 ms for R_1^{auto} . For the measurements at 400 MHz, the delay times were 4.3, 8.6, 13.0, 17.6, 25.9, 34.5 and 43.2 ms for R_2^{auto} and 40, 80, 160, 240, 340, 480, 680 and 900 ms for R_1^{auto}. Rate measurements at 300 MHz were performed with delays 4.0, 8.1, 12.1, 16.1, 24.2, 32.2, 40.3 and 48.4 ms for R_2^{auto} and 40, 80, 120, 160, 240, 340, 480, 680 ms for R_1^{auto}. The Carr–Purcell–Meiboom–Gill (CPMG) pulse train in the R_2^{auto} measurements was applied with a spacing of 250 μs between 180° pulses. R_1^{auto} measurements utilized proton 180° pulses at 5 ms intervals during the relaxation delays. Hard ^{1}H and ^{13}C pulses were about 10 and 18μs (600 MHz), 10 and 19 μs (400 MHz) and 9 and 17 μs (300 MHz), respectively. Relaxation rates were extracted by fitting the expression $I(T) = I(0)\exp(-T/R_{1,2}^{auto})$ to the experimental intensities. On average the level of experimental errors in the R_1^{auto} and R_2^{auto} rates were 1.8, 1.9% (600 MHz), 2.0, 2.2% (400 MHz) and 2.5, 2.8% (300 MHz), estimated from repeated measurements.

Pulse sequences described by Kojima et al. (1999) were employed to measure the longitudinal and transverse cross-correlated relaxation rates (R_1^{cross} and R_2^{cross}). Delays of $T = 9.4$, 15 and 30 ms were used for R_2^{cross} measurements and $T = 60$, 120, 180 and 240 ms were used for the R_1^{cross} measurements. Experiments 'A' to measure signals proportional to the initial coherence C_x (or Zeeman order C_z) were recorded with 32 scans while experiment 'B' which measure signals proportional to the coherence $2C_xH_z$ (or two-spin order $2C_zH_z$) resulting from CSA/dipole cross-correlation were recorded with 96 or 128 scans. Cross-correlation rates were measured by fitting the ratio of the intensities obtained in the two experiments to the expression $I_B/I_A = \tanh(R_{1,2}^{cross}T)$. The average errors in R_1^{cross} and R_2^{cross} values were 2.5, 2.3% (600 MHz), 2.8, 2.3% (400 MHz) and 3.5, 2.8% (300 MHz), respectively. The errors were estimated from the pair-wise root mean square deviations obtained by repeating the measurements.

All two-dimensional ^{13}C-^{1}H correlation spectra were acquired with 256 × 1024 points and a delay of 1.7 s between transients, with the ^{1}H carrier set on the water resonance (4.7 ppm) and the ^{13}C carrier frequency in the center of the aromatic carbon region (145 ppm). The experiments were performed at a temperature of 308 K on a 2 mM sample of the RNA kissing complex of Figure 1 in D_2O containing 100 mM NaCl, 0.1 mM EDTA and 10 mM sodium phosphate buffer at a pH of 6.5.

Results and discussion

The correlation between the measured longitudinal auto-relaxation rates R_1^{auto} and cross-correlation rates R_1^{cross} is shown in Figure 2. A similar correlation plot of the transverse relaxation rates R_2^{auto} and R_2^{cross} is shown in Figure 3. The B_0 dependence is much greater in Figure 2 since the rates are determined largely by the spectral density function $J(\omega_C)$ at the ^{13}C Larmor frequency. In Figure 3 on the other hand, the rates are dominated by $J(0)$. The spread of the data points in the two figures can be due to variations in the ^{13}C CSA tensor orientations and magnitudes, to local

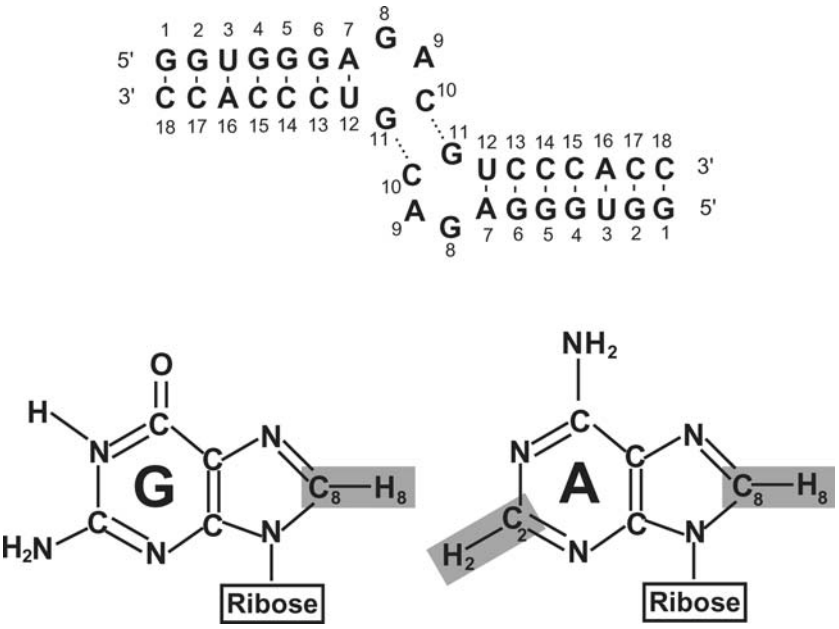

Figure 1. Schematic nucleotide sequence of the RNA kissing complex. The intermolecular Watson–Crick base pairing C10–G11 leading to dimer formation is indicated by dotted lines. The C2–H2 and C8–H8 spin systems are shown within the framework of the adenosine and guanosine units.

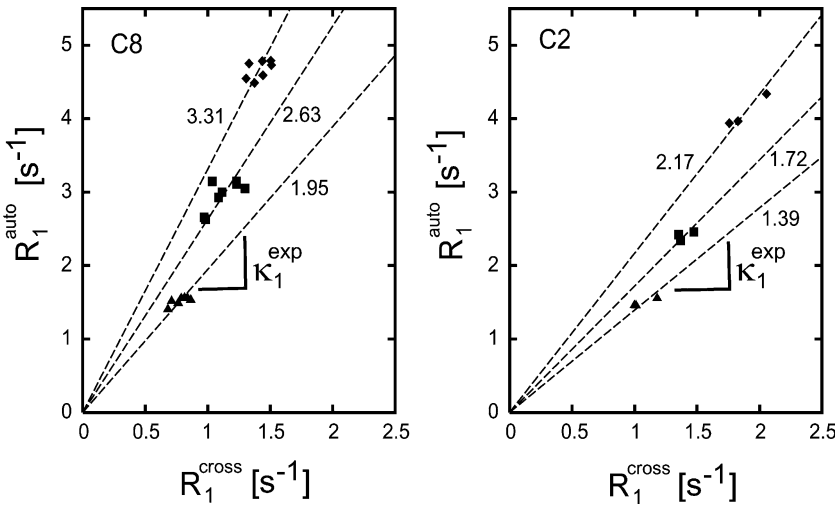

Figure 2. Correlation between R_1^{auto} and R_1^{cross} in the RNA kissing complex measured at 600 (triangles), 400 (squares) and 300 (diamonds) MHz, for C8 and C2 carbons of the purine bases. Dashed lines correspond to linear fits using relaxation data for all residues with slopes indicated in the figure.

motions and to anisotropic overall tumbling. The slopes give experimental estimates of the mean values of the ratios κ_1 and κ_2 for all observable purine C2 and C8 signals at each field. If overall tumbling were isotropic, the two ratios, κ_1 and κ_2 should be the same for a given ^{13}C CSA tensor. The dashed lines in the two figures indicate the linear fits obtained for data at three different fields, using all observable purine C2 and C8 signals. Unlike what is expected for the case of isotropic overall motion, the slopes in Figure 2 are consistently higher than those in Figure 3. This indicates

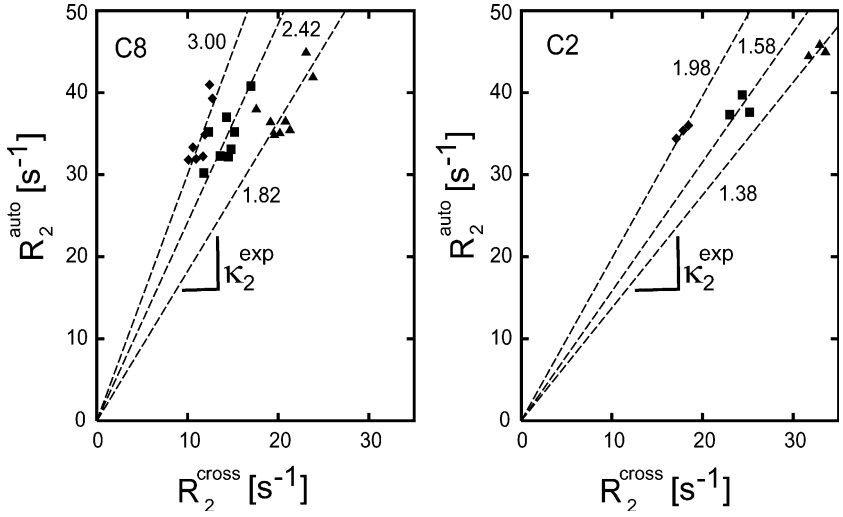

Figure 3. Correlation between R_2^{auto} and R_2^{cross} in the RNA kissing complex measured at 600 (triangles), 400 (squares) and 300 (diamonds) MHz, for C8 and C2 carbons of the purine bases. Dashed lines correspond to linear fits using relaxation data for all residues with slopes indicated in the figure.

that the dispersion of the data points cannot be only due to variations in the CSA tensors.

In Figure 4 we compare theoretical ratios κ_1 and κ_2 calculated for individual C8 carbons in the RNA kissing complex for isotropic or anisotropic overall tumbling. The ^{13}C CSA tensor magnitudes were taken from density functional calculations for C8 carbons in 9-methyl-guanine and 9-methyl-adenine (Sitkoff and Case, 1998), with the σ_{11} component oriented at an angle of 20° with respect to the C–H bond. The calculations incorporating anisotropic tumbling were carried out using $\tau_c^{iso} = 8.9$ ns and $D_{||}/D_{\perp} = 1.9$ which were determined by model-free analysis of the longitudinal and transverse auto-relaxation rates of the imino ^{15}N spins (Dittmer et al., 2003). This corresponds to $D_{||}$ and $D_{\perp}$ values of 2.74×10^7 and 1.44×10^7 s^{-1} respectively. The $D_{||}$ axis is assumed to be along the length of the complex connecting the C3′ of residue C18 of one unit to the C3′ of residue C18 of the other unit of the dimer. A C–H bond length of 0.109 nm has been employed in the calculations. The polar angles which define the orientation of the different ^{13}C–^{1}H vectors and the principal axes of the ^{13}C CSA tensors with respect to the frame of the diffusion tensor were calculated from the NMR structure of the RNA complex (Kim and Tinoco, 2000).

The two predicted ratios κ_1 and κ_2 are identical in the case of isotropic overall motion and have values of κ_1 and $\kappa_2 = 1.56$, 2.09 and 2.67 at the magnetic fields corresponding to 600, 400 and 300 MHz respectively. In the presence of motional anisotropy, the two ratios differ from each other, although both ratios remain independent of $\tau_c^{iso} = 1/6\ D_{iso}$. Calculations carried out for τ_c^{iso}values of 8.9 and 6.1 ns with $D_{||}/D_{\perp}$ fixed to 1.9 give the same values for the two ratios. Interestingly, the average of the ratios $\kappa_{av} = 1/2(\kappa_1 + \kappa_2)$ is largely independent of the extent of motional anisotropy. Using one of these ratios alone as a function of the static magnetic field in conjunction with Equation (10) would lead to errors in the estimation of CSA parameters if motional anisotropy cannot be neglected. However, the average of the two ratios, κ_{av} is very close to the ratio predicted for isotropic motion. In the presence of motional anisotropy the spectral density functions $J(\omega_C)$ and $J(0)$ deviate in opposite directions with respect to the value corresponding to isotropic rotation. Fushman and Cowburn have presented expressions for the deviation of spectral density functions $J(\omega_N)$ and $J(0)$ in the presence of motional anisotropy (Fushman and Cowburn, 1999). Simulations show that $J(\omega_N)$ and $J(0)$ deviate in opposite directions under the influence of motional anisotropy and these trends are mirrored in the relaxation rates R_1^{auto} and R_2^{auto}. Since the transverse relaxation rates are dominated by J(0) and the longitudinal rates are influenced by $J(\omega_C)$ only, the two ratios

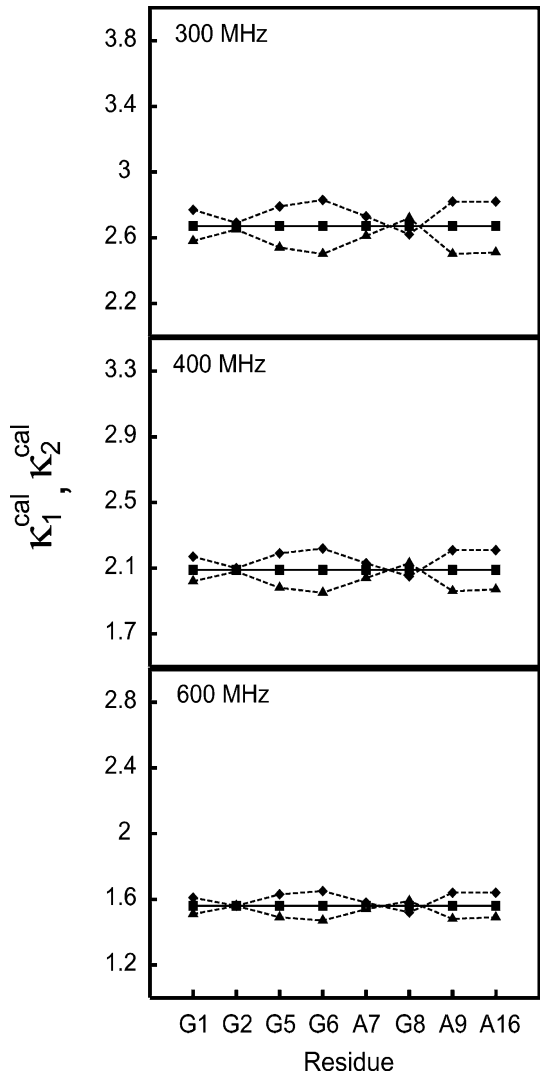

Figure 4. Ratios $\kappa_1 = R_1^{auto}/R_1^{cross}$ (diamonds connected by dashed lines) and $\kappa_2 = R_2^{auto}/R_2^{cross}$ (triangles connected by dashed lines) calculated assuming anisotropic rotational diffusion at three magnetic fields. Squares connected by the solid line, corresponds to the value calculated for isotropic overall motion and is the same for both ratios.

κ_1 and κ_2 fluctuate in opposite directions with respect to κ_{iso}. Thus the average ratio κ_{av} can be used in Equation (10) to determine CSA parameters even in the presence of motional anisotropy.

In order to examine the reliability of this approach, we have carried out calculations to determine the effect of various parameters on the ratios κ_1 and κ_2. For a given ^{13}C CSA tensor and anisotropy $D_{||}/D_{\perp}$, the two ratios are independent of the value of D_{iso}. We therefore fixed the value of $\tau_c^{iso} = 1/6D_{iso}$ to 8.9 ns and examined the effect of variations in the orientation $\theta_{11,CH}$ of the least shielded component of the CSA tensor with respect to the ^{13}C–^{1}H dipolar vector and the parameter $D_{||}/D_{\perp}$. The CSA tensor magnitudes were kept the same in all cases with the σ_{33} component of the CSA tensor perpendicular to the plane of the aromatic ring system and σ_{11} and σ_{22} lying in the plane of the ring. The results illustrated in Figure 5 refer to the C8 carbon in residue G5 which shows pronounced effects of anisotropy (see Figure 4). Similar conclusions are valid for the other residues which have C-H bonds with different orientations with respect to the long axis of the rotational diffusion tensor. The residues for which calculations have been carried out have angles between the C–H bond and the $D_{||}$ axis spanning a range of 48–115°. As $\theta_{11,CH}$ or $D_{||}/D_{\perp}$ increase, the ratios κ_1 and κ_2 deviate significantly from the values expected on the basis of Equation (10). The deviations are greater at lower magnetic fields. The average κ_{av} however is largely independent of $\theta_{11,CH}$ and $D_{||}/D_{\perp}$. Theoretical and experimental studies of CSA tensors of ^{13}C and ^{15}N nuclei in proteins and nucleic acids (or related model compounds) indicate that the angle $\theta_{11,CH}$ (or $\theta_{11,NH}$) is usually within the range of 10–30° (Sitkoff and Case, 1998; Oas et al., 1987; Yao and Hong, 2002; Haberkorn et al., 1981). In cases where the motional anisotropy $D_{||}/D_{\perp}$ is very large, even the average ratio κ_{av} can deviate from the isotropic ratio of Equation (10). Richter et al. (1999) have presented a comparison of the inertia tensors for a selection of different RNA's and proteins. Even for a highly asymmetric mass distribution, the $D_{||}/D_{\perp}$ ratio does not exceed 2.7 for both proteins and oligonucleotides. Hence in most cases, the average ratios κ_{av} are described adequately by Equation (10). The use of the average ratio κ_{av} in Equation (10) for the estimation of CSA tensor parameters has the advantage that an a priori knowledge of the molecular structure is not necessary. The only structural parameter employed in Equation (10) is the single bond C–H distance and no information about the orientation of the spin interactions with respect to the diffusion tensor is required. It maybe safely assumed that the C–H distance is the same for all the residues, since it is not involved in interactions such as hydrogen bonding which can cause variations in bond lengths.

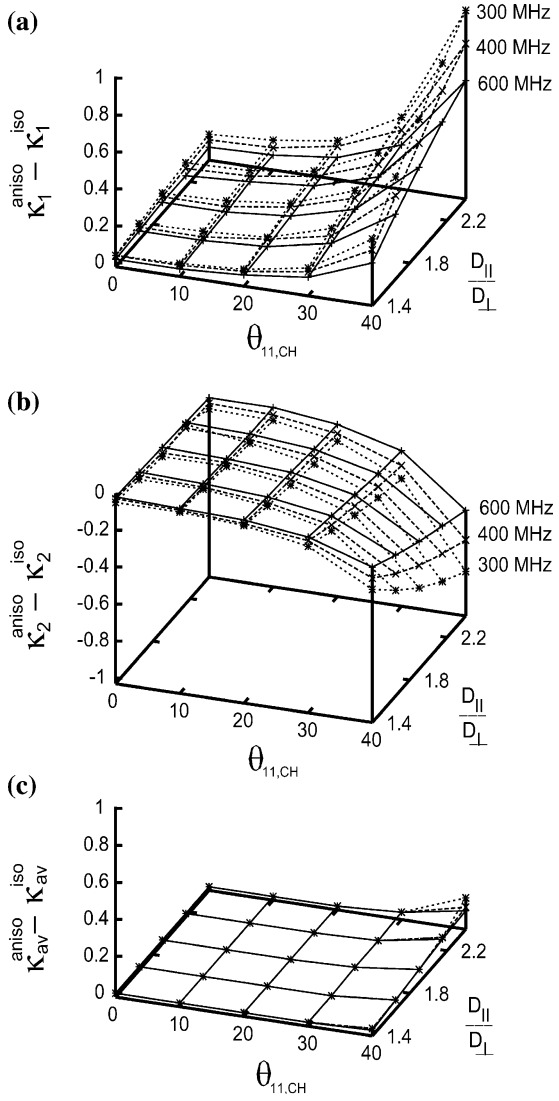

Figure 5. Deviations of ratios (a) $\kappa_1 = R_1^{auto}/R_1^{cross}$ (b) $\kappa_2 = R_2^{auto}/R_2^{cross}$ and (c) the average of the two ratios $\kappa_{av} = 1/2(\kappa_1 + \kappa_2)$ calculated assuming anisotropic overall motion from the ratio calculated assuming isotropic overall motion. The deviation is shown as a function of the orientation $\theta_{11,CH}$ of the least shielded component of the ^{13}C CSA tensor with respect to the C–H bond and the ratio of rotational diffusion constants $D_{||}/D_\perp$ at three magnetic fields.

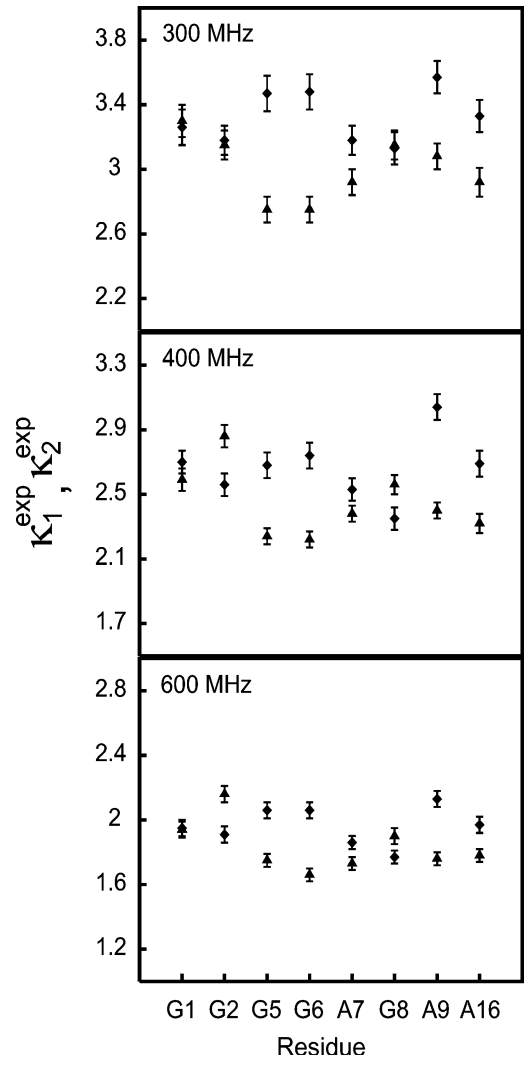

Figure 6. Ratios $\kappa_1 = R_1^{auto}/R_1^{cross}$ (diamonds) and $\kappa_2 = R_2^{auto}/R_2^{cross}$ (triangles) measured for the C8 carbons of the RNA kissing complex at three magnetic fields.

In Figure 6, we show the experimental ratios κ_1 and κ_2 obtained from relaxation rate measurements at three different magnetic fields. The observed ratios are clearly higher than the calculated ratios in Figure 4. The variation of the ratios from one nucleotide to another, however, can be ascribed to anisotropic overall motion. Residues G1 and G2 show anomalously high values for the ratio κ_2. These residues probably have conformational exchange contributions to their transverse relaxation rate (Brutscher et al., 1997). Effects of conformational fluctuations in these residues have also been observed in our earlier studies of $^{15}N/^{13}C$–^1H (CSA/dipole) cross-correlation rates in the RNA kissing complex (Ravindranathan et al., 2003).

The average κ_{av} of the measured ratios κ_1 and κ_2 have been utilized in combination with Equation (10) to obtain the CSA parameters $\Delta\sigma_{eff}$ and $\Delta\sigma^*$. The parameters for each residue were determined by fitting Equation (10) to the average of

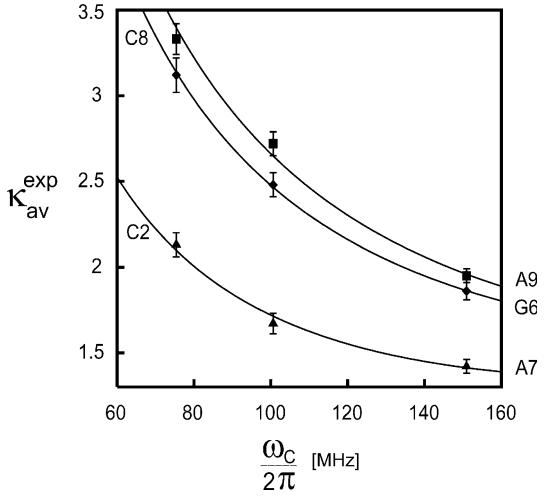

Figure 7. Examples of the fits of the average κ_{av} of the experimental ratios $\kappa_1 = R_1^{auto}/R_1^{cross}$ and $\kappa_2 = R_2^{auto}/R_2^{cross}$ measured at three fields, using Equation (10). Lines correspond to the best fits obtained by minimization of the target function in Equation (11).

the experimental ratios κ_{av}, by minimization of the target function,

$$\chi^2 = \sum_{\omega_C} \left[\frac{\kappa_{av}^{exp}(\omega_C) - \kappa_{iso}^{cal}(\omega_C)}{\delta(\omega_C)} \right]^2, \qquad (11)$$

where $\delta(\omega_C)$ is the error in κ_{av} measured at a Larmor frequency ω_C and the superscripts 'exp' and 'cal' refer to experimental ratios and ratios calculated using Equation (10), respectively. Figure 7 illustrates a few typical examples of fits of Equation (10) to averages $\kappa_{av}{}^{exp}(\omega_C)$ measured at three fields. The values of the CSA parameters $\Delta\sigma_{eff}$ and $\Delta\sigma^*$ determined from such fits are given in Table 1. Also included for comparison are the values determined from solid-state NMR studies on adenosine and guanosine and the CSA parameters obtained from density functional theory calculations (Sitkoff and Case, 1998; Stueber and Grant, 2002).

In general our measurements show that, the C2 carbons have higher $\Delta\sigma_{eff}$ and $\Delta\sigma^*$ values compared to C8. This is consistent with solid-state NMR results and DFT calculations. On average, our $\Delta\sigma_{eff}$ values are lower than the values determined by solid-state NMR. Lower effective chemical shift anisotropies in solution compared to solids have also been observed for C^{α} carbons, carbonyl carbons and aromatic carbons in side chains of proteins (Tjandra and Bax, 1997b; Pang and Zuiderweg, 2000; Damberg et al., 1999). The lowest $\Delta\sigma_{eff}$ values are observed for the residues A7, G8 and A9. The latter two residues are in the hairpin loop (see Figure 1) and the A7 residue is adjacent to this loop. Comparing the ratios κ_1 and κ_2 for these residues with the trends observed for motional anisotropy shown in Figure 4, it does not appear that the low values of these CSA parameters could have resulted from internal motions. Variations between ^{13}C CSA parameters for residues in α-helices and β-sheets in proteins suggest that such variations may be due to secondary structure (Tjandra and Bax, 1997b). More data on different RNA molecules would be needed before the CSA variations could be ascribed to secondary structural features. It should also be noted that a larger data set incorporating measurements at more magnetic field strengths would further improve the accuracy of the assessment of site-specific variations in CSA tensor parameters. This has been demonstrated recently in the case of Ubiquitin by utilizing relaxation data available at five different

Table 1. ^{13}C CSA parameters for the carbons in the purine bases of the RNA kissing complex

Residue	$\Delta\sigma_{eff}$ (ppm) (see Equation (4))	$\Delta\sigma^*$ (ppm) (see Equation (7))
	C8	
G5	133.9 ± 10.9	−81.0 ± 2.4
G6	120.1 ± 9.4	−78.9 ± 1.7
A7	112.7 ± 8.0	−79.3 ± 1.5
G8	114.5 ± 7.9	−78.4 ± 1.5
A9	108.0 ± 7.7	−72.0 ± 1.3
A16	122.2 ± 9.2	−78.6 ± 1.7
Solid state NMR[a]		
G	134.3	−91.4
A	134.3	−92.8
Ab initio[b]		
G	113.2	−89.8
A	113.6	−90.3
	C2	
A7	167.9 ± 9.3	−125.1 ± 3.4
A9	160.2 ± 9.9	−129.6 ± 3.3
A16	175.5 ± 11.3	−127.5 ± 4.3
Solid state NMR[a]		
A	178.0	−126.7
Ab initio[b]		
A	146.4	−125.5

[a]Stueber and Grant (2002).[b](Sitkoff and Case (1998).

magnetic fields. Damberg et al have discussed the optimum choice of magnetic field strength at which the ratio of auto- and cross-relaxation rates are expected to best reflect the site to site variations in the ^{15}N CSA tensor parameters (Damberg et al., 2005).

The determination of CSA parameters described above can be influenced by errors arising from approximations involved in the ratios κ_1 and κ_2. These ratios were analyzed assuming an isolated two-spin system. This is a reasonable assumption in the case of C2 and C8 in purines in RNA or DNA since the ^{13}C spins considered here are flanked by two ^{15}N spins and in general the proton density is much lower than in proteins. As discussed by Fushman et al. (1998), the ratio κ_2 is only useful for residues which do not have conformational exchange contributions R_{ex} to their relaxation rate $R_2{}^{auto}$. A further consideration is the neglect of high-frequency spectral densities that contributes to the rates $R_1{}^{auto}$ and $R_2{}^{auto}$. The transverse relaxation rate is dominated by the spectral density at zero frequency $J(0)$ so that the error in the rate $R_2{}^{auto}$ arising from the neglect of the terms $J(\omega_H+\omega_C)$, $J(\omega_H)$ and $J(\omega_H-\omega_C)$ lies within experimental error. The neglect of high-frequency terms is more significant in the case of $R_1{}^{auto}$. The longitudinal relaxation rate not only has dipolar and CSA contributions proportional to the spectral density function $J(\omega_C)$ but additional dipolar contributions due to high frequency terms $J(\omega_H+\omega_C)$ and $J(\omega_H-\omega_C)$. The contributions from the latter terms will act as a perturbation to the average ratio κ_{av} used in the determination of the CSA parameters. Setting $\omega_C \approx 1/4\omega_H$ in Equation (2) shows that in general, the contributions from the high-frequency spectral density terms to the rate $R_1{}^{auto}$ are approximately 10% of the dipolar contribution from $J(\omega_C)$. Note that the neglect of high-frequency spectral densities in $R_1{}^{auto}$ is justified only for slow tumbling at high magnetic fields and in cases of nuclei with large effective anisotropies. In order to estimate the effect of the high-frequency terms on the determination of the CSA parameters, we repeated the calculations by subtracting a correction factor of 10% from $R_1{}^{auto}$ before evaluating the average κ_{av}. This gives an upper bound of the error in the estimates of $\Delta\sigma^*$ and $\Delta\sigma_{eff}$ that can result from the neglect of high-frequency terms. The value of $\Delta\sigma^*$ increase by no more than 5% whereas the variations $\Delta\sigma_{eff}$ remain within the uncertainites indicated in Table 1. In contrast, when the CSA parameters are determined from the ratio κ_2 alone, the parameter $\Delta\sigma^*$ has deviations up to 1–17%, and $\Delta\sigma_{eff}$ deviates up to 4–14% depending on the effect of motional anisotropy at each C-H site.

The correction for high-frequency terms may also be carried out using experimental heteronuclear NOEs without making any assumptions about the ^{13}C CSA tensors (Fushman et al., 1998). This approach is similar to the reduced spectral density approach demonstrated for ^{15}N relaxation (Farrow et al., 1995). The extra contribution to the rate $R_1{}^{auto}$, which causes the slight deviation of the average ratio κ_{av} from the isotropic ratio corresponds to

$$\Delta_{corr} = \frac{d^2}{4}[6J(\omega_H+\omega_C)+J(\omega_H-\omega_C)]. \quad (12)$$

Using the expression for heteronuclear NOE (Abragam, 1961),

$$\eta_C\{H\} = 1+\left(\frac{\gamma_H}{\gamma_C}\right)\times\frac{d^2}{4R_1}[6J(\omega_H+\omega_C)-J(\omega_H-\omega_C)] \quad (13)$$

and assuming that $\omega_C \approx 1/4\omega_H$, hence $[6J(\omega_H+\omega_C)+J(\omega_H-\omega_C)] \approx 2.745\times 6J(\omega_H+\omega_C)-J(\omega_H-\omega_C)]$, the correction factor may be estimated from experimental quantities,

$$\Delta_{corr} = 2.745\left(\frac{\gamma_C}{\gamma_H}\right)(\eta_C\{H\}-1)R_1. \quad (14)$$

Subtracting this correction factor from the experimental $R_1{}^{auto}$ rates eliminates the error in the ratio κ_1. This is only required for smaller molecules where the contributions from high-frequency terms are not negligible.

The approach described here can be extended to C5-H5 and C6-H6 systems in the pyrimidine bases and to all C-H spin systems of ribose units by using fractional ^{13}C enrichment or site-specific labeling. Experiments utilizing C-C filters, which remove unwanted signals from ^{13}C-^{13}C pairs, may be applied to relaxation rate measurements in C5-H5 or C6-H6 systems (Boisbouvier et al., 1999). Mapping the CSA parameters for all accessible C-H systems should hopefully provide a correlation between ^{13}C CSA tensors and secondary structures in nucleic acids.

Conclusions

The model independent approach proposed by Fushman et al. has been extended to encompass anisotropic overall motion and applied to determine ^{13}C CSA tensor parameters for protonated carbons of purine bases in RNA. In the original approach, which assumes isotropic overall motion the ratio $\kappa_2 = R_2^{auto}/R_2^{cross}$ of the transverse auto- and cross-correlation rates provides a means to estimate CSA tensor parameters without knowledge of the parameters related to molecular dynamics. If the overall motion of the molecule is anisotropic, the ratio κ_2 is no longer independent of molecular dynamics. In such cases it is possible to utilize in addition to κ_2, the corresponding ratio $\kappa_1 = R_1^{auto}/R_1^{cross}$ of the longitudinal auto- and cross-correlation rates. The average $\kappa_{av} = 1/2\,(\kappa_1 + \kappa_2)$ of the two ratios is largely independent of motional anisotropy and may be used to estimate the CSA tensor parameters.

Acknowledgements

This work was supported by the Fonds National de la Recherche Scientifique (FNRS) and the Commission pour la Technologie et l'Innovation (CTI) of Switzerland. This work was carried out during S. R.'s stay at the Ecole Polytechnique Fédérale, Lausanne.

References

Abragam, A. (1961) *Principles of Nuclear Magnetism*, Clarendon Press, Oxford, UK.
Boisbouvier, J., Brutscher, B., Simorre, J-P. and Marion, D. (1999) *J. Biomol. NMR*, **18**, 241–252.
Boisbouvier, J., Brutscher, B., Pardi, A., Marion, D. and Simorre, J. (2000) *J. Am. Chem. Soc.*, **122**, 6779–6780.
Boyd, R. and Redfield, C. (1998) *J. Am. Chem. Soc.*, **120**, 9692–9693.
Boyd, R. and Redfield, C. (1999) *J. Am. Chem. Soc.*, **121**, 7441–7442.
Brutscher, B. (2000) *Concept. Magn. Reson.*, **12**, 207–229.
Brutscher, B., Bruschweiler, R. and Ernst, R.R. (1997) *Biochemistry*, **36**, 13043–13053.
Cisnetti, F., Loth, K., Pelupessy, P. and Bodenhausen, G. (2004) *Chem. Phys. Chem.*, **5**, 807–814.
Cornilescu, G. and Bax, A. (2000) *J. Am. Chem. Soc.*, **122**, 10143–10154.
Czernek, J. (2001) *J. Phys. Chem. A*, **105**, 1357–1365.
Czernek, J., Fiala, R. and Sklenar, V. (2000) *J. Magn. Reson.*, **145**, 142–146.
Damberg, P., Javert, J., Allard, P. and Graslund, A. (1999) *J. Biomol. NMR*, **15**, 27–37.
Damberg, P., Javert, J. and Graslund, A. (2005) *J. Am. Chem. Soc.*, **127**, 1995–2005.
Dejaegere, A.P. and Case, D.A. (1998) *J. Phys. Chem. A*, **102**, 5280–5289.
Dittmer, J., Kim, C-H. and Bodenhausen, G. (2003) *J. Biomol. NMR*, **26**, 259–275.
Farrow, N.A., Zhang, O., Szabo, A., Torchia, D.A. and Kay, L.E. (1995) *J. Biomol. NMR*, **6**, 153–162.
Fushman, D. and Cowburn, D. (1998) *J. Am. Chem. Soc.*, **120**, 7109–7110.
Fushman, D. and Cowburn, D. (1999) *J. Biomol. NMR.*, **13**, 139–147.
Fushman, D., Tjandra, N. and Cowburn, D. (1998) *J. Am. Chem. Soc.*, **120**, 10947–10952.
Ghosh, R., Marino, J.P., Wiberg, K.B. and Prestegard, J.H. (1994) *J. Am. Chem. Soc.*, **116**, 8827–8828.
Ghosh, R., Huang, K. and Prestegard, J.H. (1998) *J. Magn. Reson.*, **135**, 487–499.
Goldman, M. (1984) *J. Magn. Reson.*, **60**, 437–452.
Haberkorn, R.A., Stark, R.E., Willigen, H.van and Griffin, R.G. (1981) *J. Am. Chem. Soc.*, **103**, 2534–2539.
Kay, L.E., Nicholson, L.K., Delaglio, F., Bax, A. and Torchia, D.A. (1992) *J. Magn. Reson.*, **97**, 359–375.
Kim, C.H. and Tinoco, I. (2000) *Proc. Natl. Acad. Sci.*, **97**, 9396–9401.
Kojima, C., Ono, A., Kainosho, M. and James, T.L. (1999) *J. Magn. Reson.*, **136**, 169–175.
Oas, T.G., Hartzell, C.J., Dahlquist, F.W. and Drobny, G.P. (1987) *J. Am. Chem. Soc.*, **109**, 5962–5966.
Ottiger, M., Tjandra, N. and Bax, A. (1997) *J. Am. Chem. Soc.*, **119**, 9825–9830.
Pang, Y. and Zuiderweg, E.R.P. (2000) *J. Am. Chem. Soc.*, **122**, 4841–4842.
Ravindranathan, S., Kim, C-H. and Bodenhausen, G. (2003) *J. Biomol. NMR*, **27**, 365–375.
Richter, C., Griesinger, C., Felli, I., Cole, P.T., Varani, G. and Schwalbe, H. (1999) *J. Biomol. NMR*, **15**, 241–250.
Sitkoff, D. and Case, D.A. (1998) *Prog. Nucl. Magn. Reson. Spectrosc.*, **32**, 165–190.
Spera, S. and Bax, A. (1991) *J. Am. Chem. Soc.*, **113**, 5490–5492.
Stueber, D. and Grant, D.M. (2002) *J. Am. Chem. Soc.*, **124**, 10539–10551.
Szilagyi, L. (1995) *Prog. Nucl. Magn. Reson. Spectrosc.*, **27**, 325–443.
Tessari, M., Vis, H., Boelens, R., Kaptein, R. and Vuister, G.W. (1997) *J. Am. Chem. Soc.*, **119**, 8985–8990.
Tjandra, N., Szabo, A. and Bax, A. (1996) *J. Am. Chem. Soc.*, **118**, 6986–6991.
Tjandra, N. and Bax, A. (1997a) *J. Am. Chem. Soc.*, **119**, 8076–8082.
Tjandra, N. and Bax, A. (1997b) *J. Am. Chem. Soc.*, **119**, 9576–9577.
Wijmenga, S.S. and van Buuren, B.N.M. (1998) *Prog. Nucl. Magn. Reson. Spectrosc.*, **32**, 287–387.
Woessner, D.E. (1962) *J. Chem. Phys.*, **3**, 647–654.
Yao, X. and Hong, M. (2002) *J. Am. Chem. Soc.*, **124**, 2730–2738.